ACS central science

Research Article

Cite This: ACS Cent. Sci. 2018, 4, 1642−1651

http://pubs.acs.org/journal/acscii

Critical Assessment of the Interaction between DNA and Choline Amino Acid Ionic Liquids: Evidences of Multimodal Binding and Stability Enhancement

Dipak Kumar Sahoo,[†,‡] Subhrakant Jena,[†,‡] Juhi Dutta,[†,‡] Suman Chakrabarty,*[,§] and Himansu S. Biswal*[,†,‡]

[†]School of Chemical Sciences, National Institute of Science Education and Research, PO-Bhimpur-Padanpur, Via-Jatni, District-Khurda, PIN-752050, Bhubaneswar, India

[‡]Homi Bhabha National Institute, Training School Complex, Anushakti Nagar, Mumbai 400094, India

[§]Department of Chemical, Biological & Macromolecular Sciences, S. N. Bose National Centre for Basic Sciences, Salt Lake, Kolkata 700106, India

Supporting Information

ABSTRACT: Long-term storage and stability of DNA is of paramount importance in biomedical applications. Ever since the emergence of ionic liquids (ILs) as alternate green solvents to aqueous and organic solvents, their exploration for the extraction and application of DNA need conscientious understanding of the binding characteristics and molecular interactions between IL and DNA. Choline amino acid ILs (CAAILs) in this regard seem to be promising due to their non-cytotoxic, completely biobased and environment-friendly nature. To unravel the key factors for the strength and binding mechanism of CAAILs with DNA, various spectroscopic techniques, molecular docking, and molecular dynamics simulations were employed in this work. UV−Vis spectra indicate multimodal binding of CAAILs with DNA, whereas dye displacement studies through fluorescence emission confirm the intrusion of IL molecules into the minor groove of DNA. Circular dichorism spectra show that DNA retains its native B-conformation in CAAILs. Both isothermal titration calorimetry and molecular docking studies provide an estimate of the binding affinity of DNA with CAAILs ≈ 4 kcal/mol. The heterogeneity in binding modes of CAAIL-DNA system with evolution of time was established by molecular dynamics simulations. Choline cation while approaching DNA first binds at surface through electrostatic interactions, whereas a stronger binding at minor groove occurs via van der Waals and hydrophobic interactions irrespective of anions considered in this study. We hope this result can encourage and guide the researchers in designing new bio-ILs for biomolecular studies in future.

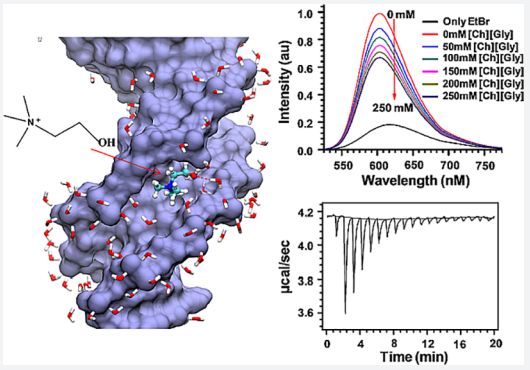

INTRODUCTION

Nucleic acids (DNA and RNA) have become an active field of research because of their biological significance as genetic information carrier. DNA is used as microarrays for gene expression analyses and as detector for single nucleotide polymorphism.[1,2] Research on DNA has also extended to nanotechnology as a powerful tool in molecular transport devices, molecular computing devices, and molecular motors.[3−7] In addition, DNA bestows the suitable condition for protein synthesis.[8] Nucleic acids are not stable in aqueous solutions at room temperature for long periods (months) due to degradation of nucleobases and inherent chemical instability.[9−11] DNA in aqueous solutions denatures easily at non-physiological temperature, pH, and ionic strength, and small volumes of aqueous solutions at high temperature under open air condition undergo evaporation causing constraint to the DNA storage.[9] Therefore, long-term storage of DNA at room temperature and its functionality in nanotechnology needs attention of solvents free of aqueous buffers.

At the end of 20th century, ionic liquids (ILs) were considered as attractive alternatives to water and organic solvents due to their distinctive properties like low vapor pressure, low toxicity, high thermal and chemical stabilities, inflammability, and high conductivity.[12−14] These remarkable features of ILs have made them applicable to various fields such as separation,[15,16] synthesis,[17] catalysis,[17−19] electrochemistry,[20,21] dissolution,[22] etc. Two parameters of ILs to be exploited highly for the interaction of IL with biomacromolecules are low cytotoxicity and high biodegradability. Many research groups have studied the interaction of room-temperature ionic liquids (RTILs) with DNA considering the above two parameters. Currently, the explanation of binding

Received: August 25, 2018
Published: December 4, 2018

DOI: 10.1021/acscentsci.8b00601
ACS Cent. Sci. 2018, 4, 1642−1651

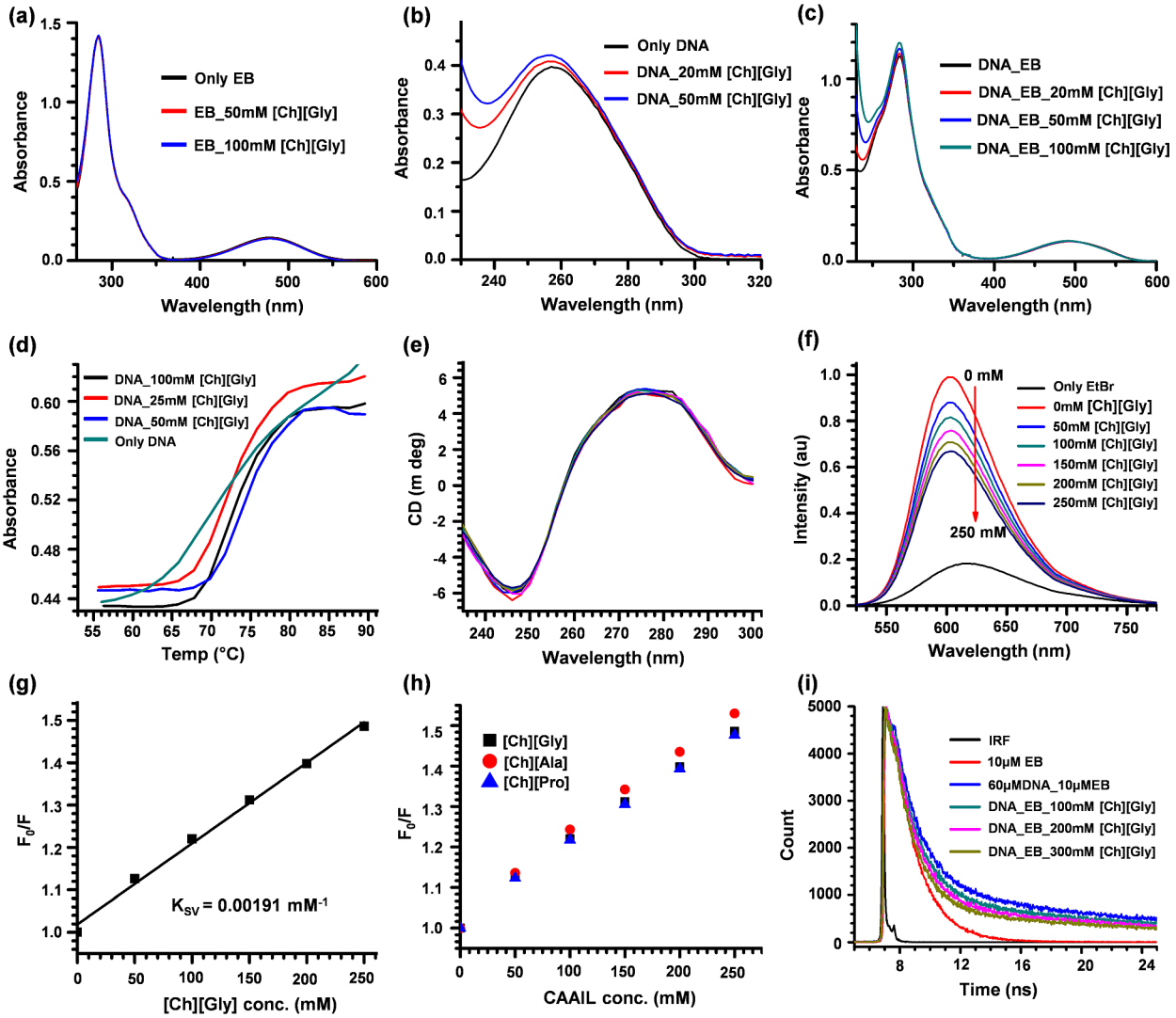

Figure 1. (a) Absorption spectra of free EB (10 μM) and EB-[Ch] [Gly] system varying the amount of ILs (50 mM and 100 mM) to a fixed concentration of EB (10 μM). (b) Absorption spectra of free DNA(60 μM) and DNA-[Ch] [Gly] system varying the amount of ILs (20 and 50 mM) to a fixed concentration of DNA (60 μM). (c) Absorption spectra of DNA-bound EB (10 μM EB, 60 μM DNA) in absence and presence of varying amounts of IL. (d) Melting curves of ct-DNA in buffer alone and 25, 50, and 100 mM [Ch] [Gly] IL. (e) CD spectra of 6.0×10^{-5} mol/L DNA in phosphate buffer (10 mM, pH 7.0) and with increasing concentrations of [Ch][Gly] from 5 to 100 mM. (f) Emission spectra of free EB (10 μM), DNA-bound EB (10 μM, 60 μM DNA), and EB-DNA-[Ch] [Gly] system varying the amount of ILs (50 to 250 mM) to a fixed concentration of DNA-bound EB (10 μM, 60 μM DNA). (g) Stern−Volmer plot for [Ch] [Gly] IL. (h) Stern−Volmer plot for all three CAAILs. (i) Fluorescence decay profiles of free EB, EB-DNA in buffer, and EB-DNA system in the presence of 100, 200, and 300 mM [Ch] [Gly] IL.

mechanism of IL with DNA is controversial. Cheng et al.[23] in their article suggested that cationic part of [Bmim] [PF_6] intercalates inside the DNA base pairs, whereas Ding et al.[24] later explained that both electrostatic and hydrophobic interactions play crucial role in DNA-[Bmim] [Cl] IL binding. Hazra et al.[25] reported another IL guanidinium tris-(pentafluoroethyl) trifluorophosphate (Gua-IL), where cationic headgroup interacts with negatively charged phosphate backbone of DNA that helps in compaction of DNA structure. Samanta et al.[26] in their spectroscopic and molecular docking study, reported groove binding of calf thymus (ct)-DNA by Morpholinium ILs. Prasad et al.[27] studied choline-based bio-ionic liquids choline glycolate and choline pyruvate for long-lasting structural and chemical stabilities of DNA, where they mentioned that significant hydrogen bonding and electrostatic interactions between DNA and ILs are responsible for this stability. While studying influence of ILs on DNA-ethidium bromide (EB) complex, Maiti et al.[28] claimed, choline-based bio-ionic liquids enhance the stability of DNA than imidazolium-based ILs, and the mode of binding between DNA and choline-based ILs (choline lactate and choline acetate) were considered to be multimodal. Recently bio-ILs like cholinium chloride, cholinium dihydrogen citrate, and cholinium bicarbonate have been reported by Khan et al. for biomolecular interactions, where they found electrostatic interactions through the minor groove.[29] Traditionally used imidazolium and pyridinium-based ILs are neither biodegradable nor non-cytotoxic.[30,31] They contain mostly halides and are obtained from nonrenewable sources and hence not ideal choice for biomolecular applications.[32] Thus, the quest for bio-ILs with less cytotoxicity is highly demanding and challenging, and the ambiguity in the mode of interactions needs to be unclouded by further detailed studies. In this regard, another class of bio-ILs, namely, choline amino acid ILs (CAAILs) like choline

DOI: 10.1021/acscentsci.8b00601
ACS Cent. Sci. 2018, 4, 1642−1651

glycine [Ch] [Gly], choline alanine [Ch][Ala], and choline proline [Ch] [Pro], are found to be promising being synthesized based on the principles of green chemistry.[33] In the CAAILs, the cationic part choline being an essential micronutrient is nontoxic and biodegradable, and the anionic part amino acids are naturally abundant, have stable chiral centers, and are not expensive.[32] Molecular structures of both cation and anions are shown in Figure S4. The advantages in the synthesis of CAAILs are their byproduct water which can be used completely, and low cost of CAAILs compared to imidazolium-based ILs and other bio-based ILs prioritizes its application in biomolecular sciences.[34−36] Recently synthesized CAAILs have been used mostly in catalysis, old paper preservation,[37] biosensor,[38] and proton conduction,[39,40] but their importance in biomolecular (DNA, RNA) interactions has not been explored in detail. Hence this study is aimed at systematic understanding of DNA−CAAIL interaction by deploying many spectroscopic techniques, namely, UV−vis absorption, steady-state fluorescence, time-resolved fluorescence, DNA melting study, circular dichorism (CD), and scanning electron microscopy (SEM). Thermodynamics of DNA−IL interaction was studied with isothermal titration calorimetry (ITC) experiment, and the mode of binding was established by molecular docking and molecular dynamics (MD) simulations.

In addition, ethidium bromide (EB) and 4′,6-diamidino-2-phenylindole (DAPI) dyes (see Figure S4) were used that bind with DNA as intercalator and groove binder, respectively, to have a comparative understanding of the unique interaction of DNA with CAAILs. We hope this work will provide intriguing physical insights on the role of bio ILs for safe storage and application of DNA.

RESULTS AND DISCUSSION

UV−Vis Spectroscopy. UV−Vis absorption measurement is one of the simplest but efficacious methods for investigating the DNA-IL interaction. Any change in position and absorbance maximum of the DNA in its bound and unbound form with ligand (IL in this case) is an indication of DNA−IL interaction, and the mode and strength of binding can also be determined from the shift.[41−46] Covalent and noncovalent binding are the two types of binding modes possible for DNA−IL complex.[45] Hyperchromism with red shift (bathochromism) in absorption maxima is the characteristic of covalent binding.[47] Noncovalent binding is further classified into intercalative, electrostatic, and groove binding. Hypochromism with bathochromism is indicative of intercalative binding,[48] whereas lower hypochromicity without bathochromic shift is indicative of electrostatic,[49] and groove binding is characterized by no or minor change in UV−vis spectra.[29,50] Hyper- and hypochromicities with moderate blue shift of the absorption band can be an indication of more than one type of interaction leading to the formation of DNA−ligand adducts.[29,45,51] Figure 1a and Figure S5b show absorption spectra of EB dye and DAPI dye with their complexes with 50 and 100 mM [Ch] [Gly] IL, respectively. Similar nature of all the three spectra indicates no binding between EB and IL. As depicted in Figure 1b, while measuring absorbance of DNA at 260 nm, hyperchromism with moderate blue shift (3−4 nm) was observed from free DNA to DNA with 50 mM [Ch] [Gly] IL. This indicates the possibility of more than one type of interaction between DNA−IL complexes. Hypochromic and bathochromic shift of EB−DNA complex from EB as observed in Figure S5a indicates intercalative binding of EB with DNA. Groove binding of DAPI to DNA is also shown in Figure S5c. Figure 1c shows effect of addition of different concentrations of [Ch] [Gly] IL with fixed concentration of DNA−EB complex. Minor change noticed in the absorption spectra of added IL to DNA−EB complex is due to preferential binding of IL with DNA (groove binding) but not with EB. Similar binding pattern is also observed in case of DNA-DAPI-IL system as shown in Figure S5d.

DNA Melting Study. UV melting experiment was performed to monitor the thermal stability of ct-DNA in absence and presence of IL. Absorbance of ct-DNA at 260 nm shows hyperchromism effect with increase in temperature due to denaturation of double-stranded DNA to single-stranded DNA caused by unstacking of nucleobases during melting process.[52] A plot of DNA absorbance at 260 nm as a function of temperature (melting curve) in the absence and presence of various quantities of [Ch] [Gly] is shown in Figure 1d. The melting points of DNA in absence and presence of different concentrations of ILs were determined from the first derivative of absorbance ([Ch] [Gly] as an example is shown in Supporting Information S13). The melting temperature of ct-DNA in the absence of IL is found to be 69.5 °C. In presence of 25 and 50 mM [Ch] [Gly] IL, the melting temperature rises to 72.4 and 74.3 °C, respectively; however, at 100 mM [Ch] [Gly] IL concentration, DNA melting point decreases to 73 °C. This shows that low concentration of CAAILs may increase DNA thermal stability, although high concentration can be effective as well. Our finding is supported by a recent simulation study by Garai et al. that shows significant increase in persistence length and stretch modulus of DNA with higher concentration of ILs.[53] The increased rigidity of DNA would result into a higher melting point (mp) as observed here. Melting curves of ct-DNA in the presence of [Ch][Ala], [Ch][Leu], and [Ch][Pro] ILs are shown in Supporting Information Figures S6a, S14, and S7a. DNA melting point increases 4−5 °C in the presence of [Ch] [Gly], [Ch][Leu], and [Ch][Ala], while it decreases 1−2 °C in the presence of [Ch][Pro]. This small decrease in melting point cannot be regarded as thermal instability; even larger decrease in mp temperatures after addition of ILs is reported,[25] where IL is found to be effective for storage of DNA. The opposite behavior of [Ch][Pro] than [Ch][Gly], [Ch][Ala], [Ch][Leu] and other aliphatic chain CAAILs could be due to different interaction patterns within ILs as explained by Gontrani et al.[34,35,39] These DNA melting results cannot be attributed to groove binding only; rather, the possibility of other modes of noncovalent bindings are expected.[8]

Circular Dichroism. CD spectrum is a useful technique to study conformational changes of optically active substances. In the CD spectrum the B form of DNA has two characteristic peaks, one positive band with maximum at 276 nm due to $\pi-\pi$ base stacking and one negative band with maximum at 246 nm due to helicity.[54] Figure 1e shows the CD spectra of ct-DNA at various concentrations of [Ch][Gly]. As can be noticed from the spectra, upon addition of increased concentration of IL from 0 to 100 mM, no conformational changes were observed in both the positive and negative bands of B form DNA. Very minute changes in the spectra as observed at higher concentration cannot be attributed to a drastic DNA conformational transition. CD spectra of DNA with increased concentration of [Ch][Ala] and [Ch][Pro] are also observed

DOI: 10.1021/acscentsci.8b00601
ACS Cent. Sci. 2018, 4, 1642−1651

similar to [Ch][Gly] and depicted in Supporting Information Figures S6b and S7b. These unaltered CD spectra show the stability of DNA in choline amino acid ILs with noncovalent interaction. We performed measurements with the same samples one month later, and the results do not suggest any time-dependent conformational changes of DNA on addition of IL (Figure S8, Supporting Information). Thus, it is confirmed that DNA retains its conformation in the presence of choline amino acid ILs.

Steady-State and Time-Resolved Fluorescence. Steady-state fluorescence is routinely used as a powerful technique to characterize the nature of interaction of DNA with small molecules. Since DNA and CAAILs are not fluorescent, suitable fluorophore can be used for the same. DAPI and EB (Figure S4) are the two fluorophores that are used in this study for dye displacement assay experiments. These two fluorophores enhance the fluorescence intensity significantly upon binding to DNA compared to their free form. Addition of increasing amount of ILs to this DNA−dye complex can be useful to determine the mode of interaction between IL and DNA. DAPI is a minor groove binder whereas EB is an intercalator to DNA. The steady-state fluorescence spectra of EB−DNA and DAPI−DNA with increasing amounts of [Ch][Gly] are shown in Figure 1f and Figure S10a, respectively. The decrease in fluorescence intensities of both EB-DNA and DAPI-DNA systems with an increase in the concentration of IL is observed. From UV−vis spectra it is known that CAAILs do not bind with EB and DAPI. This indicates that [Ch][Gly] displaces the EB and DAPI molecules from their complexes with DNA. Dye displacement studies of EB-DNA-CAAILs for other two ILs as depicted in Supporting Information Figure S9a,c show similar results. Fluorescence quenching constant K_{SV} was calculated using Stern−Volmer equation for DNA-EB and DNA-DAPI systems taking CAAILs as quencher. K_{SV} for DNA-EB fluorescence emission with [Ch][Gly], [Ch][Ala], and [Ch][Pro] as quencher are 0.001 91, 0.002 08, and 0.001 87 mM^{-1}, respectively, first one being shown in Figure 1g and all three in Figure 1h. K_{SV} values for all three CAAILs are very close, which indicates strengths of binding are similar for all CAAILs. Since all three CAAILs have the same cation, the anion of IL has negligible role in binding with DNA. Emission spectra with K_{SV} values for DNA-DAPI with all three CAAILs as quencher are shown in Figure S10. Thus, dye displacement study confirms that CAAILs bind at minor groove of DNA as intercalator and groove binder.

Lifetime measurements for both EB and DAPI dyes complexes with DNA were performed while changing IL concentration. The fluorescence decay profiles of EB−DNA as a function of the concentration of [Ch] [Gly] are shown in Figure 1i, and similar decay profiles were also observed for other two ILs given in Supporting Information S11. The estimated decay parameters for EB-DNA and [Ch] [Gly] system are provided in Table 1. They were obtained from exponential fits, $I(t) = a_1 \exp(-t/\tau 1) + a_2 \exp(-t/\tau 2) + a_3 \exp(-t/\tau_3)$, where τ_1, τ_2, and τ_3 are individual lifetime components, and a_1, a_2, and a_3 are the associated amplitudes. Fluorescence decay of only EB is found to be single exponential with lifetime of 1.62 ns, and for EB-DNA the it is biexponential with lifetimes of 1.59 and 18.73 ns. The two lifetimes in EB-DNA system are due to two forms of EB-DNA bound system in absence of [Ch] [Gly] IL. In presence of IL, a short-lived third component appeared, which remains consistent with increasing concentration of IL like fluorescence emission titration. This clearly indicates the release of EB from DNA bound state by IL. Similar observations were obtained for other two ILs system as presented in Supporting Information. From similar observations of three ILs with same cation and different anions considered in this study, one could safely conclude that anions have negligible effects on DNA binding phenomena. Thus, both UV−vis and fluorescence studies clearly imply that $[Ch]^+$ binds to DNA through intercalation as well as groove binding. The detailed binding pattern will be explained through molecular docking and MD simulations in the following section.

Table 1. Fluorescence Decay Parameters (lifetimes in ns) of Free EB, EB-DNA in Buffer, and EB-DNA System in the Presence of 100, 200, and 300 mM [Ch] [Gly] IL

sample	$\tau_1(a_1)$	$\tau_2(a_2)$	$\tau_3(a_3)$	χ^2
EB only	1.62(1.00)			1.25
EB-DNA-0 mM [Ch] [Gly]	1.59(0.27)	18.73(0.73)		1.12
EB-DNA-100 mM [Ch] [Gly]	1.58(0.30)	19.60(0.69)	0.12(0.01)	1.00
EB-DNA-300 mM [Ch] [Gly]	1.50(0.33)	19.42(0.66)	0.10(0.01)	1.05
EB-DNA-500 mM [Ch] [Gly]	1.47(0.35)	19.46(0.63)	0.10(0.01)	1.08

Thermodynamic Behavior of Interaction between Ionic Liquid and DNA-EB System. ITC was employed to investigate the thermodynamics of ILs binding with ctDNA-EB. ITC experiments were performed for the three choline amino acid ILs of 100 mM concentration each. ct-DNA (70 μM) was maintained in the ITC cell and titrated with gradual addition of EB from the syringe, until EB concentration reached more than 10 times that of ctDNA in the cell. The integrated heat data of ctDNA-EB in absence and presence of the [Ch] [Gly] IL are shown in Figure 2 and for [Ch] [Ala], [Ch] [Pro] in Supporting Information Figure S12. The thermodynamic parameters like stoichiometry (N), binding constant (K_b), enthalpy change (ΔH), entropy change (ΔS), and free energy change or binding affinity (ΔG) were obtained from fitted data in each titration and are listed in Table 2. The fitting was done with single binding site model with acceptable χ^2 value, and a good quality fitting was obtained for 100 mM IL concentration. This concentration is sufficient to give thermodynamics of DNA-EB-IL system as evidenced from steady-state and time-resolved dye displacement fluorescence study. Stoichiometry of binding in presence and absence of ILs were found to be close to 0.5, which matches with reported binding stoichiometry of ct-DNA-EB.[28,55] Stoichiometry for binding of [Ch] [Ala] is found to be lowest, that is, 0.36 among other CAAILs. Binding affinity K_b for DNA-EB system in absence of CAAILs is 5.81×10^5 mol^{-1}, which decreased to 1.25×10^5, 1.05×10^5, and 0.96×10^5 mol^{-1} in the presence of [Ch] [Gly], [Ch] [Ala], and [Ch] [Pro] ILs, respectively. Clearly, the binding affinities of CAAILs with ct-DNA are almost of equal strength irrespective of different anions; however, their binding affinities almost reduced to 1/5th that of EB. This is in consequence with weaker noncovalent binding of ILs with DNA than that of EB binding to ct-DNA as observed in UV−vis and fluorescence emission studies. If we compare the thermodynamic parameters in Table 2, DNA-EB system in absence of ILs has favorable ΔG (−7.87 kcal mol^{-1}), with more favorable enthalpic contribution ΔH (−6.61 kcal

DOI: 10.1021/acscentsci.8b00601
ACS Cent. Sci. 2018, 4, 1642−1651

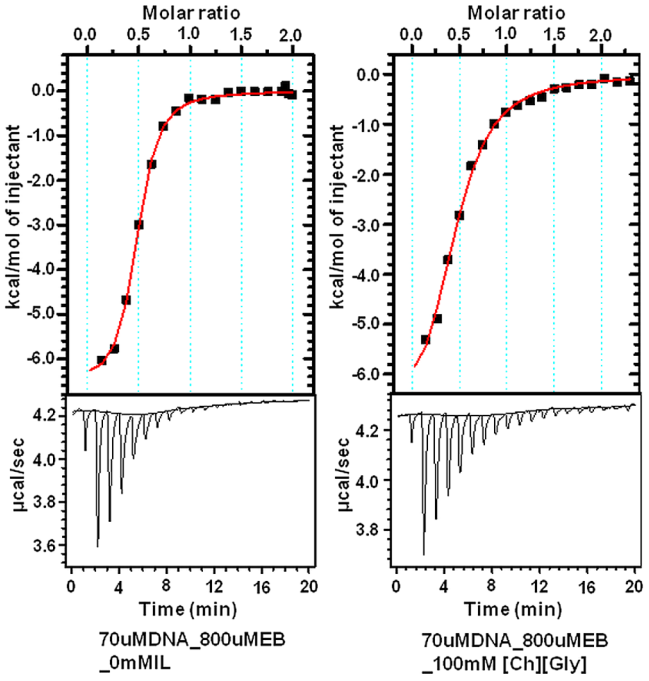

Figure 2. ITC isotherms of EB-DNA binding in buffer and in the presence of 100 mM [Ch] [Gly] IL. (bottom) Experimental data. (top) Obtained by converting the results into molar heats and plotted against the EB to ct-DNA molar ratio.

mol^{-1}) and less favorable entropic contribution $T\Delta S$ (1.26 kcal mol^{-1}). However, in the DNA-EB system in the presence of [Ch] [Gly] IL, ΔG remains favorable (ca. −6.9 kcal mol^{-1}), but there is unfavorable entropic contribution $T\Delta S$ of −0.45 kcal mol^{-1}. Similar phenomena were also observed for DNA-EB system in the presence of other two AAILs with minor reduction in ΔG values. Thus, in the presence of CAAILs, the system becomes more structured leading to decrease in entropy. Maiti et al. have attributed this phenomenon to the displacement of water from the spine of hydration by groove binding of choline cation in the minor groove forming a DNA-IL-EB complex surrounded by structured water molecules.[28] In addition, recent simulation study by Garai et al. shows significant increase in the persistence length of DNA (hence, higher rigidity) at higher concentration of ILs.[53] On the basis of our data, binding of CAAILs with ct-DNA is exothermic and primarily enthalpy driven with contributions from electrostatic as well as hydrophobic interactions at the minor groove, vide infra.

Microscopic View: Field Emission Scanning Electron Microscopy Study. DNA-IL interaction morphology can be probed by field emission scanning electron microscopy (FE-SEM). All the FE-SEM samples were prepared in phosphate (10 mM, pH 7.0) buffer. As shown in Figure 3a, DNA appears

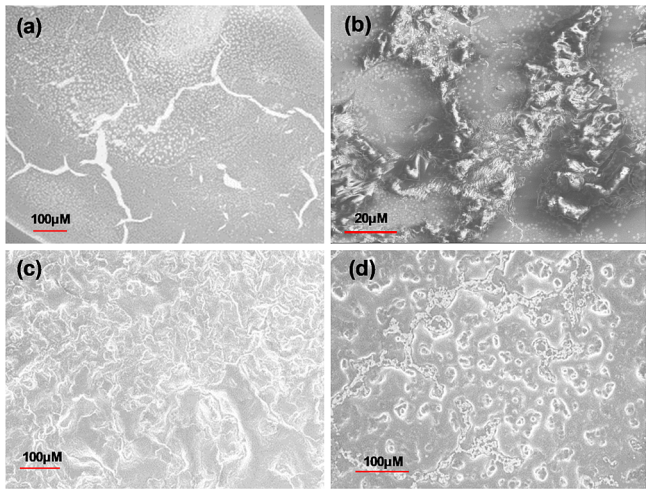

Figure 3. Microscopic FE-SEM images (a) only 60 μM ct-DNA in 10 mM phosphate buffer, (b) 60 μM ct-DNA in the presence of 60 mM [Ch] [Gly], (c) 60 μM ct-DNA in the presence of 60 mM [Ch] [Ala], (d) 60 μM ct-DNA in the presence of 60 mM [Ch] [Pro].

in coiled form in buffer alone. With the addition of 60 mM CAAILs, the coiled structure changed to different morphology with different binding pattern as shown in Figure 3b−d. Similar aggregation pattern of IL with DNA was observed for [Ch] [Ala] and [Ch] [Pro] (Figure 3c,d), whereas a little stronger aggregation is observed in case of [Ch] [Gly] (Figure 3b) as indicated in ITC study. This change is minute, which does not affect the binding strength and is consistent with the statement that anions of CAAILs have negligible effect on binding to DNA.

Molecular Docking Studies. Molecular docking can be used to gain insight into the mode and strength of biomolecular interaction at the molecular level.[56−60] In the present work, we tried to interpret the binding mechanism and strength of CAAIL with DNA through molecular docking studies by using AutoDock Vina program.[61] EB dye was also tested with DNA-CAAIL to correlate with the ITC experimental data. When CAAIL and EB were docked separately with ct-DNA, both prefer to bind at minor groove of DNA as revealed from the energetically most favorable conformation of the docked pose (Figure 4a,b). All three CAAILs [Ch][Gly], [Ch][Ala], [Ch][Pro] were docked separately with DNA, but in all cases cholinium ion binds through the minor groove of DNA irrespective of anion as inferred by fluorescence emission and ITC studies. The binding energy of the docked structure (Figure 4a) was found to be −3.9 kcal/mol for all three DNA-CAAIL interacting systems. Similar to ITC result, −7.4 and −6.8 kcal/mol binding energies were obtained for DNA-EB (Figure 4b) and DNA-EB-CAAIL (Figure 4c) , respectively. Similar results from ITC

Table 2. ITC Experimental Data Obtained from Fitting of Molar Heats Plotted against the EB to ct-DNA Molar Ratio in Absence and Presence of CAAILs

concentration of [Ch][AA] in EB-DNA	N	$K_b \times 10^5$ mol^{-1}	ΔH kcal mol^{-1}	$T\Delta S$ kcal mol^{-1}	ΔG kcal mol^{-1}
0 mM [Ch] [AA]	0.45 ± 0.01	5.81 ± 0.47	−6.61	1.26	−7.87
100 mM [Ch] [Gly]	0.45 ± 0.01	1.25 ± 0.13	−7.41	−0.45	−6.96
100 mM [Ch] [Ala]	0.36 ± 0.01	1.05 ± 0.10	−8.75	−1.90	−6.85
100 mM [Ch] [Pro]	0.41 ± 0.01	0.96 ± 0.05	−7.51	−0.71	−6.8

DOI: 10.1021/acscentsci.8b00601
ACS Cent. Sci. 2018, 4, 1642−1651

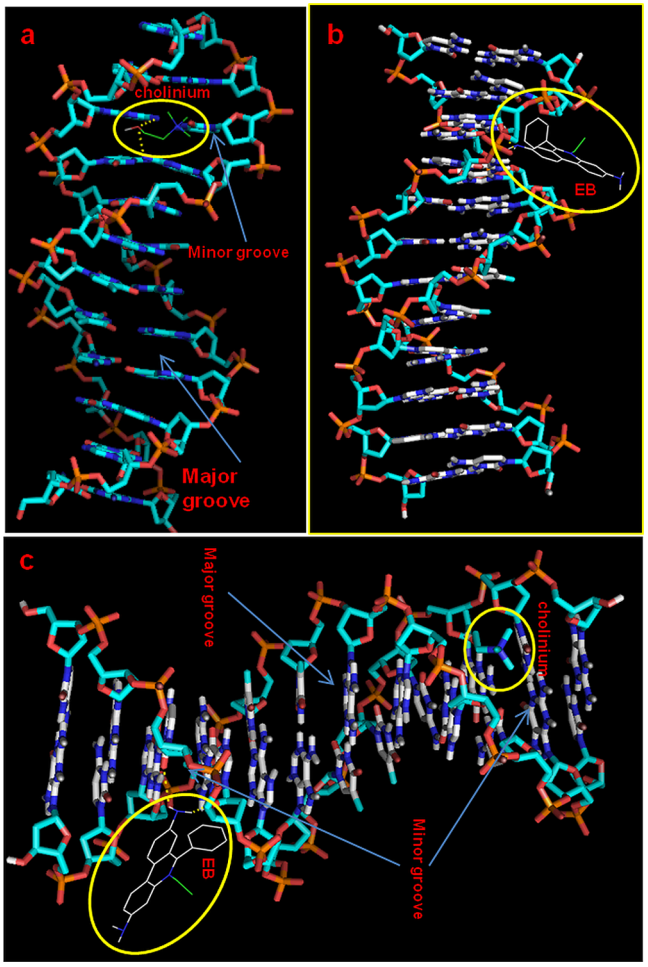

Figure 4. Molecular docking (a) cholinium ion interaction at minor groove of DNA, (b) EB interaction at minor groove of DNA, (c) both EB and cholinium interact at minor groove of DNA.

and docking studies reveal that the binding energy of DNA-CAAIL interacting system (−3.9 kcal/mol) as obtained from docking result is reliable. In DNA-CAAIL interaction, the O−H of cholinium ion forms O−H···N hydrogen bonds with DNA bases and alkyl groups of cholinium binds with DNA through hydrophobic interaction. The low value of interaction (−3.9 kcal/mol) is productive, since it will ameliorate in extraction of DNA.

To check the purity level of extracted DNA from IL solution, we followed the extraction process as per the cited method.[62] More than 80% DNA was recovered from IL solution with high purity. Purity was tested with both UV−vis and CD spectra (see Figures S15 and S16). The ratios of absorbance from 260 to 280 nm for both standard and purified DNA were found to be more than 1.8, which shows high purity level of DNA. CD spectra of purified DNA also show no change in conformer of DNA. The decrease in binding energy of DNA-EB interaction with addition of CAAIL is the result of weak noncovalent bonding of CAAIL with DNA compared to EB. Thus, on the basis of the experimental and docking results, it can be concluded that the cationic part of the CAAILs irrespective of anions interacted through minor grooves and formed electrostatic hydrogen bonds as well as hydrophobic interaction.

Molecular Dynamics Studies. The MD simulation of the DNA-CAAIL ligand system in aqueous medium was performed to investigate the structural dynamics of the DNA−ligand interaction, as well as the relative population of various modes of binding of the ligand. Mojca et al.[63] in their recent article showed the influence of charge density of ionene in the stability of DNA and found negligible effect of ionene anion on DNA binding by combined study of experimental and theoretical calculation. Chandran et al.[9] through spectroscopic and MD simulation results suggest that electrostatic, hydrophobic, and polar interactions of IL cations play significant role in DNA stability. In this work, we elucidate the binding mechanism of CAAILs with DNA using 400 ns long simulation trajectory. During the 400 ns simulation the CAAIL cation frequently approaches the DNA surface and often binds the minor groove. In Figure 5, we monitored various structural

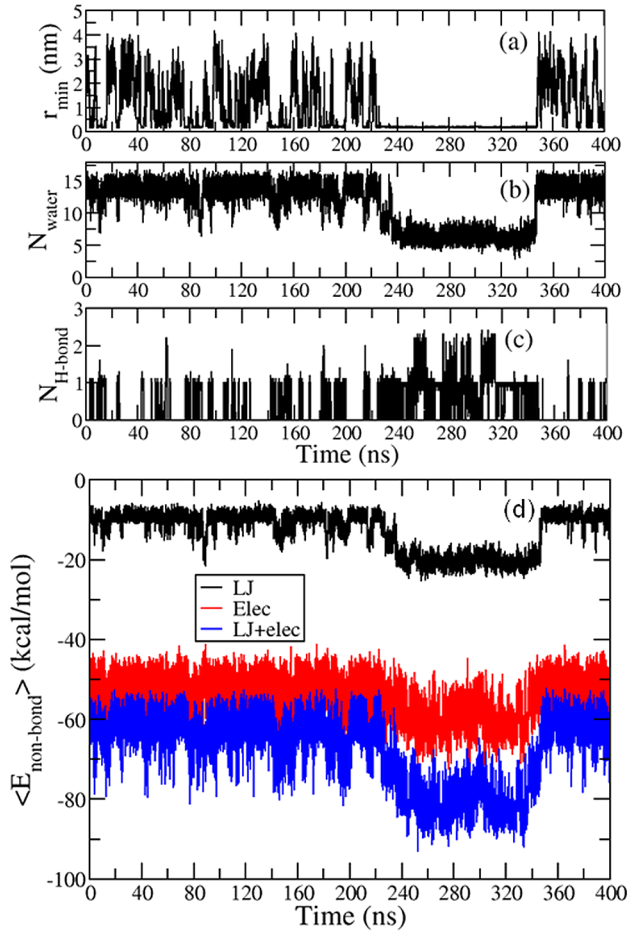

Figure 5. Time evolution of (a) the minimum (proximal) distance between DNA and the CAAIL cation, where r_{min} < 0.3 nm signifies ligand being at the DNA surface, (b) number of water molecules within 0.3 nm of the CAAIL cation, where large values indicate fully solvated ligand in the bulk water phase, and lower values (<10) signify a desolvated buried state, and (c) number of hydrogen bonds between the DNA and CAAIL cation. (d) Time evolution of the nonbonded interaction energies between CAAIL cation and its surrounding. The Lennard-Jones (LJ) and electrostatic (Elec) interactions were calculated with everything else (including DNA, water, and ions) within a 2 nm cutoff radius of the cation. The black, red, and blue lines depict the LJ, electrostatic, and total energy, respectively. The data were locally averaged over 20 ps stretch for obtaining smoother curves.

DOI: 10.1021/acscentsci.8b00601
ACS Cent. Sci. 2018, 4, 1642−1651

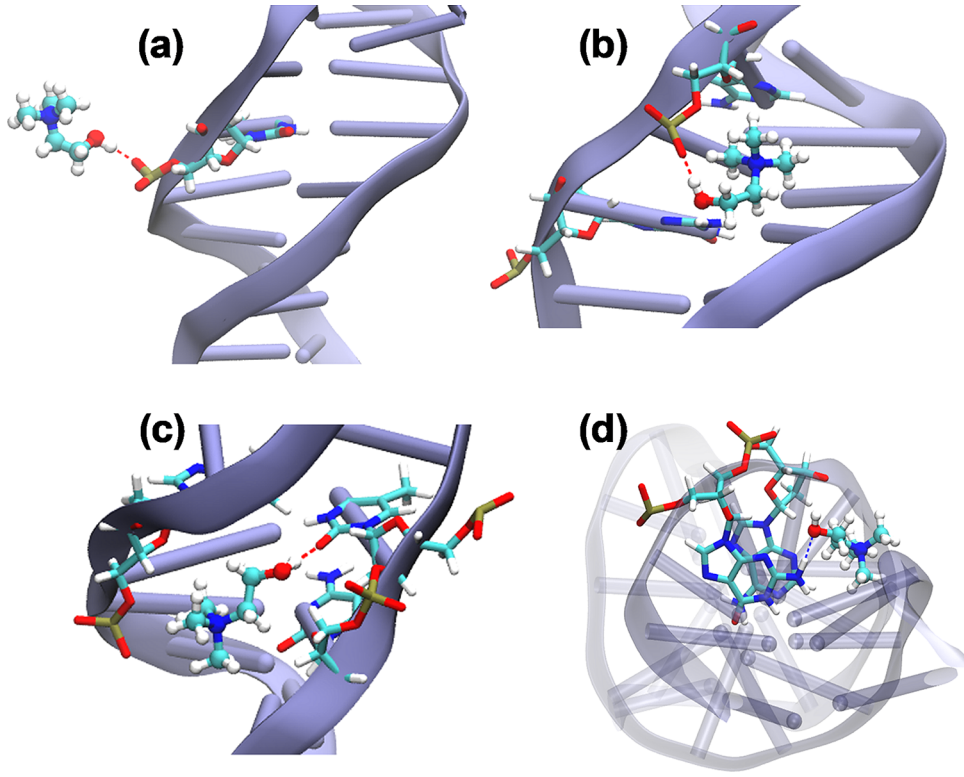

Figure 6. Representative snapshots of dominant binding modes of CAAIL cation with DNA. (a) A state where the cation binds to the DNA surface through H-bonding interaction with the phosphate group. (b−d) Depictions of various possible H-bonded interactions while the cation is deeply buried in the minor groove.

and thermodynamic parameters with time to dissect the nature of the DNA-IL interactions. Figure 5a shows the time evolution of minimum (proximal) distance (r_{min}) between the DNA and ligand. Very small values (r_{min} < 0.3 nm) indicate the ligand being very close to the DNA surface or being bound to it. During the first ∼230 ns the ligand attaches and detaches to the DNA surface intermittently, but it is found to be strongly bound to DNA during 230−350 ns. The lifetime of a bound state can vary from a few nanoseconds to 100 ns depending on the binding location signifying heterogeneity in binding mode as well as affinity.

To further elucidate the nature of the bound states, we monitored (i) the number of water molecules within 0.3 nm of the ligand (Figure 5b) and (ii) the number of hydrogen bonds between DNA and ligand (Figure 5c). This combined set of parameters clearly established the highly multimodal nature of the DNA-ligand interactions in agreement with the experimental results. The fluctuations in the number of water molecules show that during the first 230 ns of the trajectory the ligand stays predominantly on the surface, whereas it drops drastically during the 230−350 ns stretch, which corresponds to a deeply buried (in minor groove) desolvated state with very high lifetime (>100 ns). Figure 5c shows that, even when the ligand stays near the surface (<230 ns), there is frequent H-bond formation with DNA (mostly negatively charged phosphate groups). The number of H bonds fluctuates between 1 and 2 even in the minor groove bound stable state.

The above discussion clearly establishes the strong heterogeneity in the binding modes that include a desolvated minor groove bound state, as well as electrostatically stabilized surface bound states (H-bonded). We further dissected the various modes of binding from the simulation trajectory, and a few representative snapshots are shown in Figure 6. Figure 6a shows a representative snapshot of the surface-bound ligand, where the cation is H-bonded to the phosphate group of DNA. Figure 6b−d depicts the most dominant mode of binding in the minor groove. This is primarily dictated by the hydrophobic effects of the large size of the CAAIL cation, which tends to bury itself in the minor groove (supported by the dramatic desolvation as observed in Figure 5b). These modes are further stabilized by hydrogen bonding between the OH group of choline and either phosphate oxygen or bases of DNA.

Subsequently, we analyzed the nonbonded interactions of the cation ligand with its surrounding. Figure 5d shows the time evolution of both the short-range LJ and electrostatic interaction components. On comparison with Figure 5a−c, we can clearly establish that the minor groove bound state observed in the 230−350 ns stretch has the most favorable nonbonded interaction energy (ca. −80 kcal/mol), whereas in the fully detached (unbound) state the energy value is ca. −60 kcal/mol. Note that the intermittent appearances of the surface-bound states (<230 ns) are associated with quite favorable interaction energy due to the electrostatic interactions although not as low as the minor groove bound states. Interestingly, the LJ interactions seem to significantly contribute toward the high affinity of the minor groove bound state. Our analysis seems to indicate that the experimental measurement of binding affinity would have contributions from both the surface-bound states (with considerable electrostatic stabilization) as well as minor groove bound state stabilized by the van der Waals and hydrophobic interactions.

DOI: 10.1021/acscentsci.8b00601
ACS Cent. Sci. 2018, 4, 1642−1651

CONCLUSIONS

The binding characteristics and molecular mechanism of CAAILs with DNA were explored by various experimental techniques, molecular docking, and molecular dynamics simulation. The unperturbed CD spectra of DNA with increasing concentration of CAAILs and MD simulation results confirm the stability of DNA with no conformational change in DNA. The molecular interactions of ILs at minor groove of DNA via electrostatic, hydrogen bonding, and hydrophobic interactions were revealed through UV−vis spectra, fluorescence dye displacement study, molecular docking, and MD simulations. From ITC and molecular docking study, binding energy of EB dye with DNA is found to be ∼8 kcal/mol, which decreased to ∼7 kcal/mol with addition of ILs. This indicates extrusion of EB from DNA binding site by IL and weaker binding of IL with DNA. The low binding energy (4 kcal/mol) of CAAILs with DNA can be useful in back extraction of DNA. Thermal stability of DNA was also explored with melting point experiment that seems to be promising. MD simulations show the presence of strong heterogeneity in the binding modes and nature of interactions stabilizing the various modes. There are surface-bound states stabilized by electrostatic interactions and H-bonding with the phosphate groups, as well as the minor groove bound modes stabilized by van der Waals and hydrophobic interactions predominantly. On the basis of the experimental and theoretical evidence, it is concluded that CAAILs can bind DNA through choline cation irrespective of the anions taken in this study. The significance of this study lies in the fact that CAAILs were synthesized based on the principle of green chemistry and found to be completely non-cytotoxic with useful water as byproduct. The eco-friendly and non-cytotoxic nature of CAAILs could be useful in DNA binding, their extraction, and safe storage of genetic blue prints for future and can also guide the researchers in designing new bio-ILs.

ASSOCIATED CONTENT

Supporting Information

The Supporting Information is available free of charge on the ACS Publications website at DOI: 10.1021/acscentsci.8b00601.

Details of experimental and computational methods, NMR spectra, ITC isotherms, CD Spectra, and safety statement (PDF)

AUTHOR INFORMATION

Corresponding Authors

*E-mail: himansu@niser.ac.in. Phone: +91-674-2494 185/186. (H.S.B.)

*E-mail: sumanc@bose.res.in. (S.C.)

ORCID

Suman Chakrabarty: 0000-0002-9461-0015

Himansu S. Biswal: 0000-0003-0791-2259

Notes

The authors declare no competing financial interest.

ACKNOWLEDGMENTS

The authors thank Dr. Y. S. Chaudhary and Dr. U. Subudhi for their help in carrying out some experiments in their laboratory. H.S.B. acknowledges financial support from Department of Atomic Energy, Government of India.

REFERENCES

(1) Ott, J.; Hoh, J. Set Association Analysis of Snp Case-Control and Microarray Data. *J. Comput. Biol.* **2003**, *10*, 569−574.

(2) Tateishi-Karimata, H.; Sugimoto, N. Structure, Stability and Behaviour of Nucleic Acids in Ionic Liquids. *Nucleic Acids Res.* **2014**, *42*, 8831−8844.

(3) Phadke, R. S. Biomolecular Electronics in the Twenty-First Century. *Appl. Biochem. Biotechnol.* **2001**, *96*, 269−276.

(4) Yurke, B.; Turberfield, A. J.; Mills, A. P., Jr; Simmel, F. C.; Neumann, J. L. A DNA-Fuelled Molecular Machine Made of DNA. *Nature* **2000**, *406*, 605.

(5) Li, T. I.N.G.; Sknepnek, R.; Olvera de la Cruz, M. Thermally Active Hybridization Drives the Crystallization of DNA-Functionalized Nanoparticles. *J. Am. Chem. Soc.* **2013**, *135*, 8535−8541.

(6) Girard, M.; Millan, J. A.; Olvera de la Cruz, M. DNA-Driven Assembly: From Polyhedral Nanoparticles to Proteins. *Annu. Rev. Mater. Res.* **2017**, *47*, 33−49.

(7) Wang, M. X.; Brodin, J. D.; Millan, J. A.; Seo, S. E.; Girard, M.; Olvera de la Cruz, M.; Lee, B.; Mirkin, C. A. Altering DNA-Programmable Colloidal Crystallization Paths by Modulating Particle Repulsion. *Nano Lett.* **2017**, *17*, 5126−5132.

(8) Liu, H.; Dong, Y.; Wu, J.; Chen, C.; Liu, D.; Zhang, Q.; Du, S. Evaluation of Interaction between Imidazolium-Based Chloride Ionic Liquids and Calf Thymus DNA. *Sci. Total Environ.* **2016**, *566−567*, 1−7.

(9) Chandran, A.; Ghoshdastidar, D.; Senapati, S. Groove Binding Mechanism of Ionic Liquids: A Key Factor in Long-Term Stability of DNA in Hydrated Ionic Liquids? *J. Am. Chem. Soc.* **2012**, *134*, 20330−20339.

(10) Lukin, M.; de Los Santos, C. Nmr Structures of Damaged DNA. *Chem. Rev.* **2006**, *106*, 607−686.

(11) Vijayaraghavan, R.; Izgorodin, A.; Ganesh, V.; Surianarayanan, M.; MacFarlane, D. R. Long-Term Structural and Chemical Stability of DNA in Hydrated Ionic Liquids. *Angew. Chem., Int. Ed.* **2010**, *49*, 1631−1633.

(12) He, Y.; Li, Z.; Simone, P.; Lodge, T. P. Self-Assembly of Block Copolymer Micelles in an Ionic Liquid. *J. Am. Chem. Soc.* **2006**, *128*, 2745−2750.

(13) Huddleston, J. G.; Visser, A. E.; Reichert, W. M.; Willauer, H. D.; Broker, G. A.; Rogers, R. D. Characterization and Comparison of Hydrophilic and Hydrophobic Room Temperature Ionic Liquids Incorporating the Imidazolium Cation. *Green Chem.* **2001**, *3*, 156−164.

(14) Zhou, Y.; Antonietti, M. Synthesis of Very Small Tio2 Nanocrystals in a Room-Temperature Ionic Liquid and Their Self-Assembly toward Mesoporous Spherical Aggregates. *J. Am. Chem. Soc.* **2003**, *125*, 14960−14961.

(15) Anderson, J. L.; Ding, J.; Welton, T.; Armstrong, D. W. Characterizing Ionic Liquids on the Basis of Multiple Solvation Interactions. *J. Am. Chem. Soc.* **2002**, *124*, 14247−14254.

(16) Blanchard, L. A.; Brennecke, J. F. Recovery of Organic Products from Ionic Liquids Using Supercritical Carbon Dioxide. *Ind. Eng. Chem. Res.* **2001**, *40*, 287−292.

(17) Hallett, J. P.; Welton, T. Room-Temperature Ionic Liquids: Solvents for Synthesis and Catalysis. 2. *Chem. Rev.* **2011**, *111*, 3508−3576.

(18) Olivier-Bourbigou, H.; Magna, L.; Morvan, D. Ionic Liquids and Catalysis: Recent Progress from Knowledge to Applications. *Appl. Catal., A* **2010**, *373*, 1−56.

(19) Wasserscheid, P.; Keim, W. Ionic Liquids—New "Solutions" for Transition Metal Catalysis. *Angew. Chem., Int. Ed.* **2000**, *39*, 3772−3789.

(20) Fukumoto, K.; Yoshizawa, M.; Ohno, H. Room Temperature Ionic Liquids from 20 Natural Amino Acids. *J. Am. Chem. Soc.* **2005**, *127*, 2398−2399.

(21) Leone, A. M.; Weatherly, S. C.; Williams, M. E.; Thorp, H. H.; Murray, R. W. An Ionic Liquid Form of DNA: Redox-Active Molten Salts of Nucleic Acids. *J. Am. Chem. Soc.* **2001**, *123*, 218−222.

DOI: 10.1021/acscentsci.8b00601
ACS Cent. Sci. 2018, 4, 1642−1651

(22) Phillips, D. M.; Drummy, L. F.; Conrady, D. G.; Fox, D. M.; Naik, R. R.; Stone, M. O.; Trulove, P. C.; De Long, H. C.; Mantz, R. A. Dissolution and Regeneration of Bombyx Mori Silk Fibroin Using Ionic Liquids. *J. Am. Chem. Soc.* **2004**, *126*, 14350−14351.
(23) Cheng, D. H.; Chen, X. W.; Wang, J. H.; Fang, Z. L. An Abnormal Resonance Light Scattering Arising from Ionic-Liquid/DNA/Ethidium Interactions. *Chem. - Eur. J.* **2007**, *13*, 4833−4839.
(24) Ding, Y.; Zhang, L.; Xie, J.; Guo, R. Binding Characteristics and Molecular Mechanism of Interaction between Ionic Liquid and DNA. *J. Phys. Chem. B* **2010**, *114*, 2033−2043.
(25) Satpathi, S.; Sengupta, A.; Hridya, V. M.; Gavvala, K.; Koninti, R. K.; Roy, B.; Hazra, P. A Green Solvent Induced DNA Package. *Sci. Rep.* **2015**, *5*, 9137.
(26) Pabbathi, A.; Samanta, A. Spectroscopic and Molecular Docking Study of the Interaction of DNA with a Morpholinium Ionic Liquid. *J. Phys. Chem. B* **2015**, *119*, 11099−11105.
(27) Sharma, M.; Mondal, D.; Singh, N.; Trivedi, N.; Bhatt, J.; Prasad, K. High Concentration DNA Solubility in Bio-Ionic Liquids with Long-Lasting Chemical and Structural Stability at Room Temperature. *RSC Adv.* **2015**, *5*, 40546−40551.
(28) Mishra, A.; Ekka, M. K.; Maiti, S. Influence of Ionic Liquids on Thermodynamics of Small Molecule−DNA Interaction: The Binding of Ethidium Bromide to Calf Thymus DNA. *J. Phys. Chem. B* **2016**, *120*, 2691−2700.
(29) Haque, A.; Khan, I.; Hassan, S. I.; Khan, M. S. Interaction Studies of Cholinium-Based Ionic Liquids with Calf Thymus DNA: Spectrophotometric and Computational Methods. *J. Mol. Liq.* **2017**, *237*, 201−207.
(30) Docherty, K. M.; Kulpa, C. F., Jr. Toxicity and Antimicrobial Activity of Imidazolium and Pyridinium Ionic Liquids. *Green Chem.* **2005**, *7*, 185−189.
(31) Bernot, R. J.; Brueseke, M. A.; Evans-White, M. A.; Lamberti, G. A. Acute and Chronic Toxicity of Imidazolium-Based Ionic Liquids on Daphnia Magna. *Environ. Toxicol. Chem.* **2005**, *24*, 87−92.
(32) Liu, Q.-P.; Hou, X.-D.; Li, N.; Zong, M.-H. Ionic Liquids from Renewable Biomaterials: Synthesis, Characterization and Application in the Pretreatment of Biomass. *Green Chem.* **2012**, *14*, 304−307.
(33) De Santis, S.; Masci, G.; Casciotta, F.; Caminiti, R.; Scarpellini, E.; Campetella, M.; Gontrani, L. Cholinium-Amino Acid Based Ionic Liquids: A New Method of Synthesis and Physico-Chemical Characterization. *Phys. Chem. Chem. Phys.* **2015**, *17*, 20687−20698.
(34) Campetella, M.; De Santis, S.; Caminiti, R.; Ballirano, P.; Sadun, C.; Tanzi, L.; Gontrani, L. Is a Medium-Range Order Pre-Peak Possible for Ionic Liquids without an Aliphatic Chain? *RSC Adv.* **2015**, *5*, 50938−50941.
(35) Campetella, M.; Bodo, E.; Caminiti, R.; Martino, A.; D'Apuzzo, F.; Lupi, S.; Gontrani, L. Interaction and Dynamics of Ionic Liquids Based on Choline and Amino Acid Anions. *J. Chem. Phys.* **2015**, *142*, 234502.
(36) Campetella, M.; Bodo, E.; Montagna, M.; De Santis, S.; Gontrani, L. Theoretical Study of Ionic Liquids Based on the Cholinium Cation. Ab Initio Simulations of Their Condensed Phases. *J. Chem. Phys.* **2016**, *144*, 104504.
(37) Scarpellini, E.; Ortolani, M.; Nucara, A.; Baldassarre, L.; Missori, M.; Fastampa, R.; Caminiti, R. Stabilization of the Tensile Strength of Aged Cellulose Paper by Cholinium-Amino Acid Ionic Liquid Treatment. *J. Phys. Chem. C* **2016**, *120*, 24088−24097.
(38) Zappi, D.; Caminiti, R.; Ingo, G. M.; Sadun, C.; Tortolini, C.; Antonelli, M. L. Biologically Friendly Room Temperature Ionic Liquids and Nanomaterials for the Development of Innovative Enzymatic Biosensors. *Talanta* **2017**, *175*, 566−572.
(39) Campetella, M.; Montagna, M.; Gontrani, L.; Scarpellini, E.; Bodo, E. Unexpected Proton Mobility in the Bulk Phase of Cholinium-Based Ionic Liquids: New Insights from Theoretical Calculations. *Phys. Chem. Chem. Phys.* **2017**, *19*, 11869−11880.
(40) Gontrani, L. Choline-Amino Acid Ionic Liquids: Past and Recent Achievements About the Structure and Properties of These Really "Green" Chemicals. *Biophys. Rev.* **2018**, *10*, 873−880.
(41) Sun, H.; Xiang, J.; Liu, Y.; Li, L.; Li, Q.; Xu, G.; Tang, Y. A Stabilizing and Denaturing Dual-Effect for Natural Polyamines Interacting with G-Quadruplexes Depending on Concentration. *Biochimie* **2011**, *93*, 1351−1356.
(42) Jaumot, J.; et al. Experimental Methods for Studying the Interactions between G-Quadruplex Structures and Ligands. *Curr. Pharm. Des.* **2012**, *18*, 1900−1916.
(43) Wei, C.; Wang, J.; Zhang, M. Spectroscopic Study on the Binding of Porphyrins to (G4t4g4)4 Parallel G-Quadruplex. *Biophys. Chem.* **2010**, *148*, 51−55.
(44) Bhadra, K.; Kumar, G. S. Interaction of Berberine, Palmatine, Coralyne, and Sanguinarine to Quadruplex DNA: A Comparative Spectroscopic and Calorimetric Study. *Biochim. Biophys. Acta, Gen. Subj.* **2011**, *1810*, 485−496.
(45) Sirajuddin, M.; Ali, S.; Badshah, A. Drug-DNA Interactions and Their Study by Uv-Visible, Fluorescence Spectroscopies and Cyclic Voltametry. *J. Photochem. Photobiol., B* **2013**, *124*, 1−19.
(46) Palchaudhuri, R.; Hergenrother, P. J. DNA as a Target for Anticancer Compounds: Methods to Determine the Mode of Binding and the Mechanism of Action. *Curr. Opin. Biotechnol.* **2007**, *18*, 497−503.
(47) Nakamoto, K.; Tsuboi, M.; Strahan, G. D. Drug-DNA Interactions: Structures and Spectra. *Methods Biochem. Anal.* **2008**, *51*, 1−366.
(48) Arjmand, F.; Parveen, S.; Afzal, M.; Toupet, L.; Ben Hadda, T. Molecular Drug Design, Synthesis and Crystal Structure Determination of CuII−SnIV Heterobimetallic Core: DNA Binding and Cleavage Studies. *Eur. J. Med. Chem.* **2012**, *49*, 141−150.
(49) Song, Y.; Zhong, D.; Luo, J.; Tan, H.; Chen, S.; Li, P.; Wang, L.; Wang, T. Binding Characteristics and Interactive Region of 2-Phenylpyrazolo[1,5-C]Quinazoline with DNA. *Luminescence* **2014**, *29*, 1141−1147.
(50) Kumar, C. V.; Turner, R. S.; Asuncion, E. H. Groove Binding of a Styrylcyanine Dye to the DNA Double Helix: The Salt Effect. *J. Photochem. Photobiol., A* **1993**, *74*, 231−238.
(51) Zhao, L.; Yao, Y.; Li, S.; Lv, M.; Chen, H.; Li, X. Cytotoxicity and DNA Binding Property of Triphenylethylene−Coumarin Hybrids with Two Amino Side Chains. *Bioorg. Med. Chem. Lett.* **2014**, *24*, 900−904.
(52) Rehman, S. U.; Sarwar, T.; Husain, M. A.; Ishqi, H. M.; Tabish, M. Studying Non-Covalent Drug−DNA Interactions. *Arch. Biochem. Biophys.* **2015**, *576*, 49−60.
(53) Garai, A.; Ghoshdastidar, D.; Senapati, S.; Maiti, P. K. Ionic Liquids Make DNA Rigid. *J. Chem. Phys.* **2018**, *149*, 045104.
(54) Zhang, G.; Hu, X.; Pan, J. Spectroscopic Studies of the Interaction between Pirimicarb and Calf Thymus DNA. *Spectrochim. Acta, Part A* **2011**, *78*, 687−694.
(55) Ren, J.; Jenkins, T. C.; Chaires, J. B. Energetics of DNA Intercalation Reactions. *Biochemistry* **2000**, *39*, 8439−8447.
(56) Ali, I.; Haque, A.; Saleem, K.; Hsieh, M. F. Curcumin-I Knoevenagel's Condensates and Their Schiff's Bases as Anticancer Agents: Synthesis, Pharmacological and Simulation Studies. *Bioorg. Med. Chem.* **2013**, *21*, 3808−3820.
(57) Saleem, K.; Wani, W. A.; Haque, A.; Lone, M. N.; Hsieh, M.-F.; Jairajpuri, M. A.; Ali, I. Synthesis, DNA Binding, Hemolysis Assays and Anticancer Studies of Copper(II), Nickel(II) and Iron(III) Complexes of a Pyrazoline-Based Ligand. *Future Med. Chem.* **2013**, *5*, 135−146.
(58) Ali, I.; et al. Supramolecular Chiro-Biomedical Aspect of &#946-Blockers in Drug Development. *Curr. Drug Targets* **2014**, *15*, 729−741.
(59) Anthwal, A.; et al. Synthesis of 4-Piperidone Based Curcuminoids with Anti-Inflammatory and Anti-Proliferation Potential in Human Cancer Cell Lines. *Anti-Cancer Agents Med. Chem.* **2016**, *16*, 841−851.
(60) Naz, H.; Khan, P.; Tarique, M.; Rahman, S.; Meena, A.; Ahamad, S.; Luqman, S.; Islam, A.; Ahmad, F.; Hassan, M. I. Binding Studies and Biological Evaluation of β-Carotene as a Potential

DOI: 10.1021/acscentsci.8b00601
ACS Cent. Sci. 2018, 4, 1642−1651

Inhibitor of Human Calcium/Calmodulin-Dependent Protein Kinase Iv. *Int. J. Biol. Macromol.* **2017**, *96*, 161−170.
(61) Trott, O.; et al. AutoDock Vina: Improving the Speed and Accuracy of Docking with a New Scoring Function, Efficient Optimization, and Multithreading. *J. Comput. Chem.* **2009**, *31*, 455−461.
(62) Singh, N.; Sharma, M.; Mondal, D.; Pereira, M. M.; Prasad, K. Very High Concentration Solubility and Long-Term Stability of DNA in an Ammonium-Based Ionic Liquid: A Suitable Medium for Nucleic Acid Packaging and Preservation. *ACS Sustainable Chem. Eng.* **2017**, *5*, 1998−2005.
(63) Seručnik, M.; Podlipnik, Č.; Hribar-Lee, B. DNA−Polyelectrolyte Complexation Study: The Effect of Polyion Charge Density and Chemical Nature of the Counterions. *J. Phys. Chem. B* **2018**, *122*, 5381−5388.

DOI: 10.1021/acscentsci.8b00601
ACS Cent. Sci. 2018, 4, 1642−1651